Angewandte Chemie
Eine Zeitschrift der Gesellschaft Deutscher Chemiker

Supporting Information

Formation of Glyoxylic Acid in Interstellar Ices: A Key Entry Point for Prebiotic Chemistry

André K. Eckhardt[+], Alexandre Bergantini[+], Santosh K. Singh, Peter R. Schreiner, and Ralf I. Kaiser**

anie_201901059_sm_miscellaneous_information.pdf

Methods

Materials and Experimental Setup.

The experimental setup has been described in detail elsewhere.[1] Briefly, the simulation experiments were conducted in a contamination-free ultra-high vacuum (UHV) chamber at base pressures of a few 10^{-11} Torr.[2] Four sets of ices were prepared on a 5 ± 1 K target through deposition of the gaseous mixtures H_2O:CO, H_2O:^{13}CO, D_2O:CO, D_2O:^{13}CO at partial pressures of 8.0 ± 0.1 Torr of water and 4.0 ± 0.1 Torr of carbon monoxide, respectively. Note that the partial pressures of H_2O and CO in the gas mixing chamber were determined via calibration experiments using FTIR spectroscopy in order to achieve the final H_2O:CO ratio of 1:2. The fact that the glass capillary array retains the water molecules more effectively than the CO molecules justifies the H_2O:CO partial pressures. The ice thickness was determined to be 1000 ± 50 μm based on laser interferometry collected online during deposition.[1a] Infrared spectroscopy of the 1648 cm^{-1} (ν_2, O-H bend) and 2138 cm^{-1} (ν_1, C-O stretch) bands of water[3] and carbon monoxide,[4] respectively, determined a water to carbon monoxide ratio of (1.0:2.0) ± 0.5. The ices were irradiated with energetic electrons (5 keV) for 2 hours at 50 ± 5 nA by scanning the electron beam over an area of 1.0 ± 0.1 cm^2. According to CASINO (version 2.42) Monte Carlo[5] simulations, the samples were exposed to an average dose of 5.7 ± 0.5 eV per molecule, which is equivalent to $(5 \pm 2)\times10^7$ years of exposition to cosmic rays inside a typical molecular cloud.[6] The choice of low temperature target represents typical temperatures of ice-coated grains in cold molecular clouds; the pressure conditions of a few 10^{-11} Torr guarantee that over the time scale of each experiment of around 12 h, less than one monolayer of residual gases condensed on the icy target. For the *in situ* identification of new bands emerging, a Fourier Transform Infrared (FTIR) spectrometer (Nicolet 6700) monitored the samples during the irradiation. After the irradiation, temperature programed desorption (TPD) studies were conducted by heating the irradiated ices at a rate of 1.0 K min^{-1} to 300 K. Throughout the sublimation process, individual molecules subliming into the gas-phase were identified by ionizing the molecules via single photoionization (PI) reflectance time-of-flight mass-spectrometry (PI-ReTOF-MS). The photoionization source exploited pulsed (30 Hz) coherent vacuum ultraviolet (VUV) light in two different sets of experiments: one set at 114.6 nm (10.82 eV) and the other at 121.2 nm (10.23 eV). The VUV light was generated *via* resonant four wave mixing ($2\omega_1 - \omega_2$).[7] By systematically analyzing data from crossed isotopic experiments with D_2O and ^{13}CO, and by tuning the photoionization energy from 10.82 eV to 10.23 eV, we selectively ionized specific structural isomers based on their computed adiabatic ionization energies (IE), which enabled us to determine which isomers were produced. We would also like to discuss the source of ionizing radiation (energetic electrons). The experiments aimed at simulating the interaction of interstellar model ices with galactic cosmic rays (GCRs) to form

astrobiologically important molecules. It is very important to highlight that no laboratory experiment can simulate the interaction of the energetic GCRs with ices directly since no experimental device is accessible to the community that can generate a broad range of kinetic energies of protons and helium nuclei – the main constituents of the GCR - from the MeV to the PeV range. However, the physical effects of GCRs interacting with ices are well understood: GCR lose energy predominantly via ionization of the target molecules; the secondary electrons generated can induce further ionization thus creating electron cascades.[8] By convolving over the energies of the GCR particles, it is feasible to derive a kinetic energy distribution of the secondary electrons generated that are typically in ranges of a few eV up to the 10 keV. Therefore, rather than exposing the samples to GCR particles, we simulate the GCR processing and irradiate the samples with electrons, here at 5 keV. Their linear energy transfer (LET) is similar to LETs of 10 to 20 MeV GCR protons penetrating ices. Our ice mixtures are chosen as predominantly polar model ices, so that we could demonstrate the proof of concept that $C_2H_2O_3$ isomers can form from these mixtures upon interaction with ionizing radiation.

Computations. All computations were carried out with Gaussian 16, Revision A.03. For all geometry optimizations and frequency computations Second-order Møller–Plesset perturbation theory (MP2)[9] was employed utilizing the Dunning correlation consistent split valence basis set cc-pVTZ.[10] Based on these geometries the corresponding frozen-core coupled cluster[11] CCSD(T)/cc-pVDZ, CCSD(T)/cc-pVTZ and CCSD(T)/cc-pVQZ single point energies were computed and extrapolated to complete basis set limits,[12] CCSD(T)/CBS with MP2/cc-pVTZ zero-point vibrational energy corrections. In general, the adiabatic ionization energies were computed by taking the ZPVE corrected energy difference between the neutral and ionic species that correspond to similar conformations.

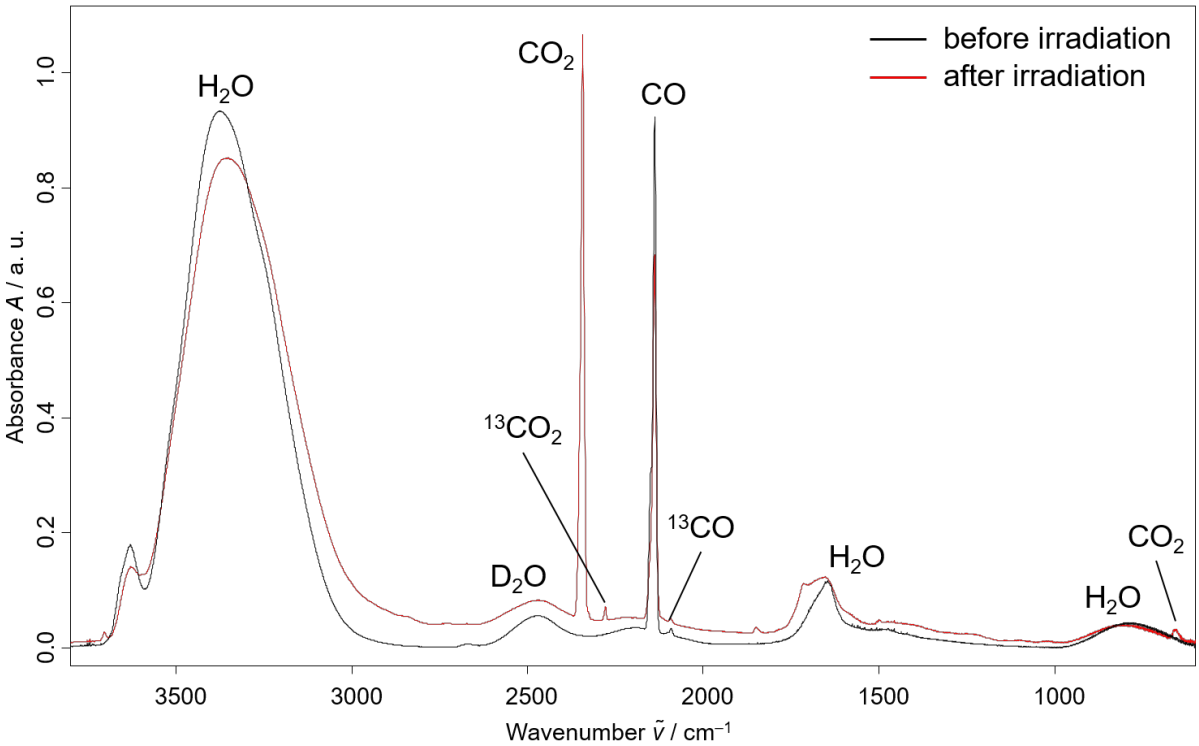

Figure S1: Recorded IR spectra of a water (H_2O) and carbon monoxide (CO) ice before (black) and after (red) 2 h electron irradiation.

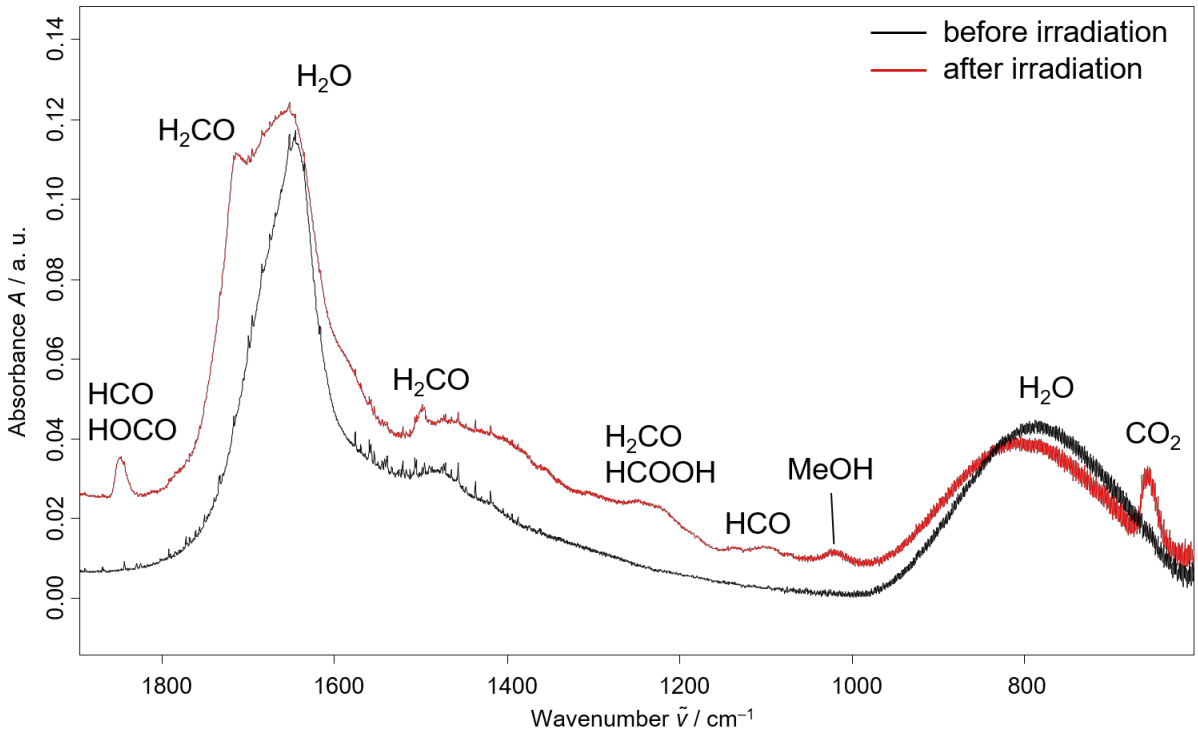

Figure S2: Recorded IR spectra of a water (H_2O) and carbon monoxide (CO) ice before (black) and after (red) 2 h electron irradiation.

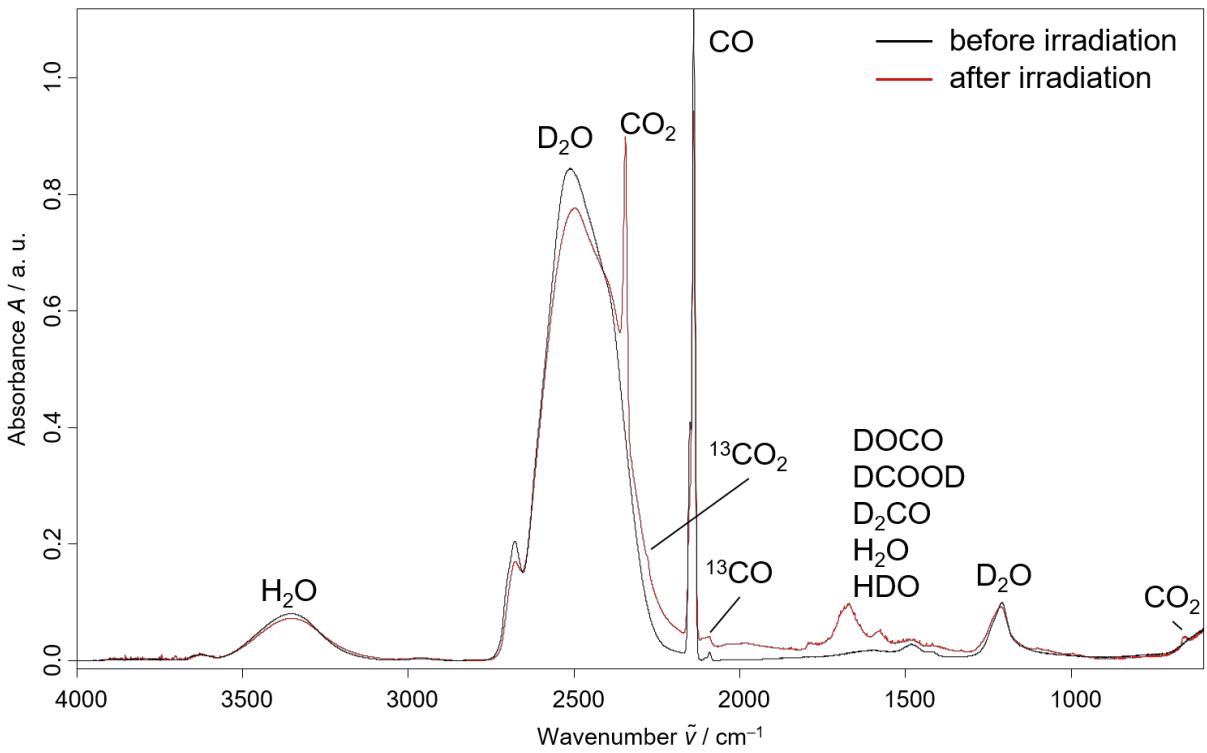

Figure S3: Recorded IR spectra of a deuterated water (D_2O) and carbon monoxide (CO) ice before (black) and after (red) 2 h electron irradiation.

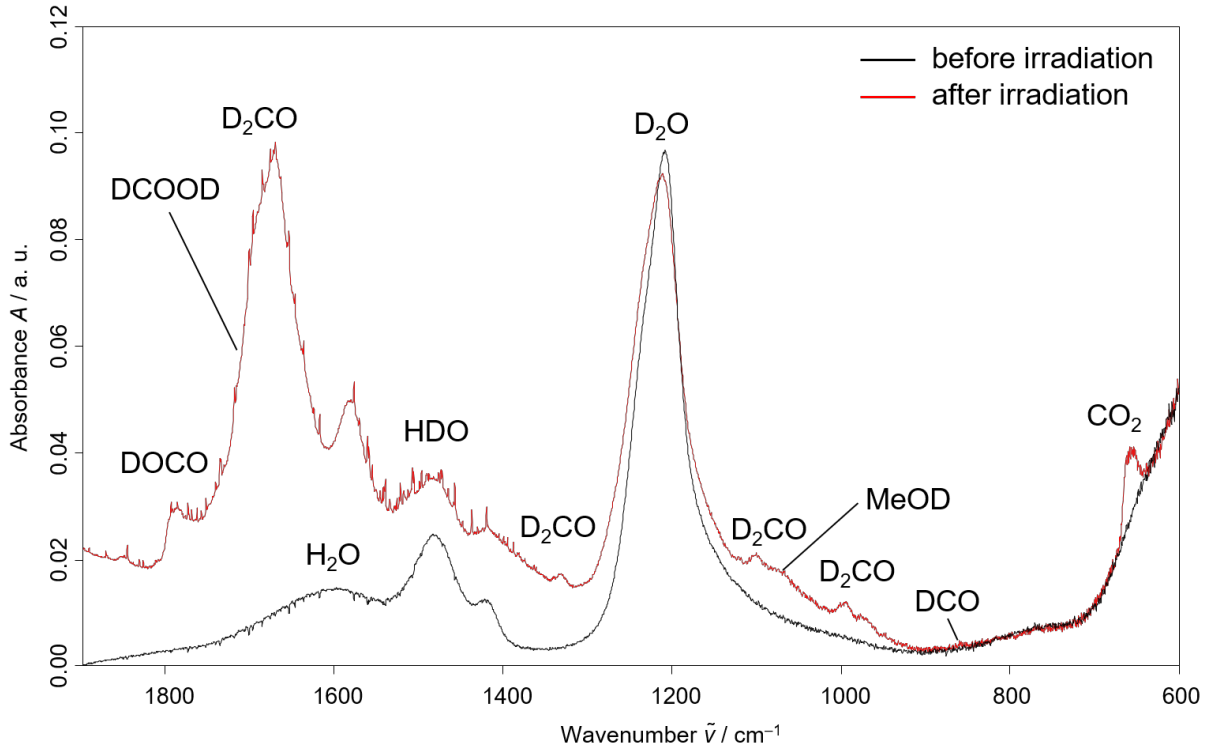

Figure S4: Recorded IR spectra of a deuterated water (D_2O) and carbon monoxide (CO) ice before (black) and after (red) 2 h electron irradiation.

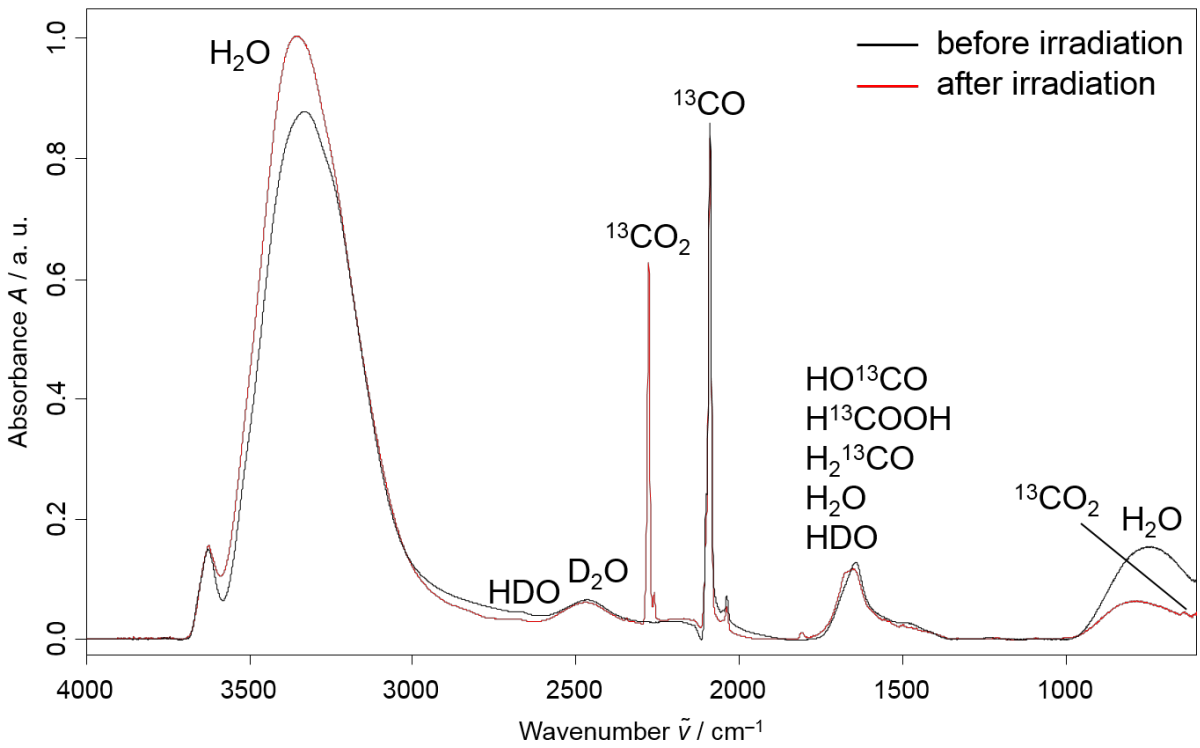

Figure S5: Recorded IR spectra of a water (H_2O) and ^{13}C-carbon monoxide (^{13}CO) ice before (black) and after (red) 2 h electron irradiation.

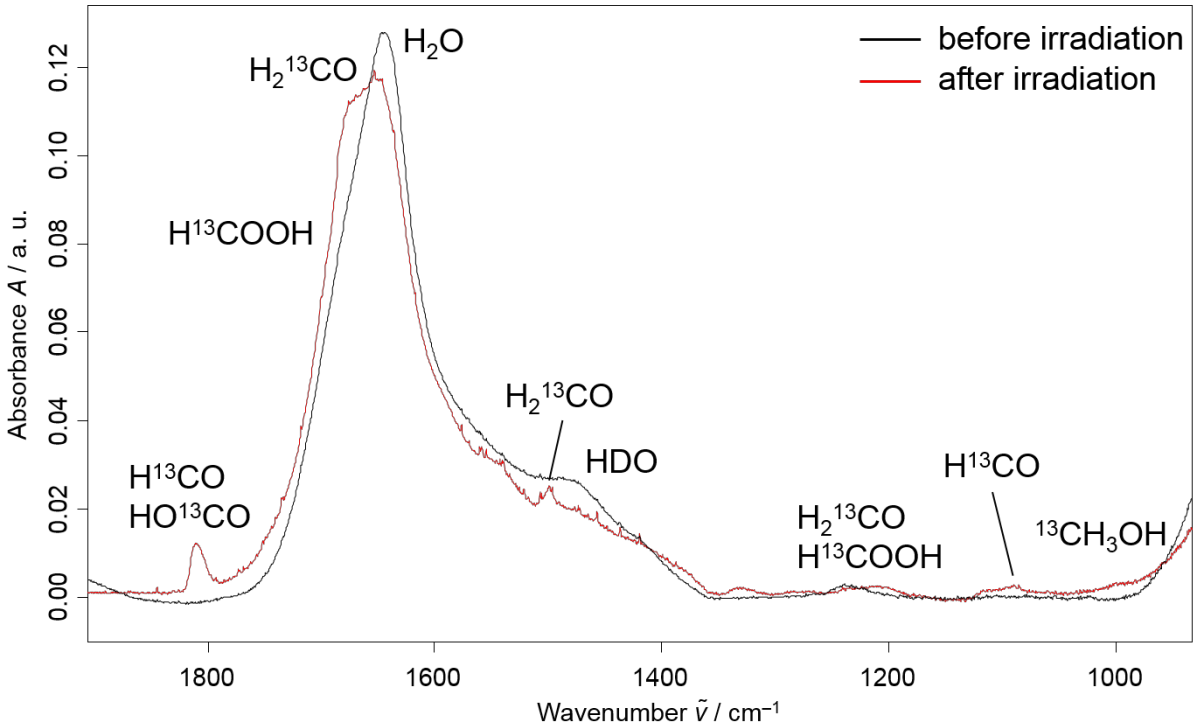

Figure S6: Recorded IR spectra of a water (H_2O) and ^{13}C-carbon monoxide (^{13}CO) ice before (black) and after (red) 2 h electron irradiation.

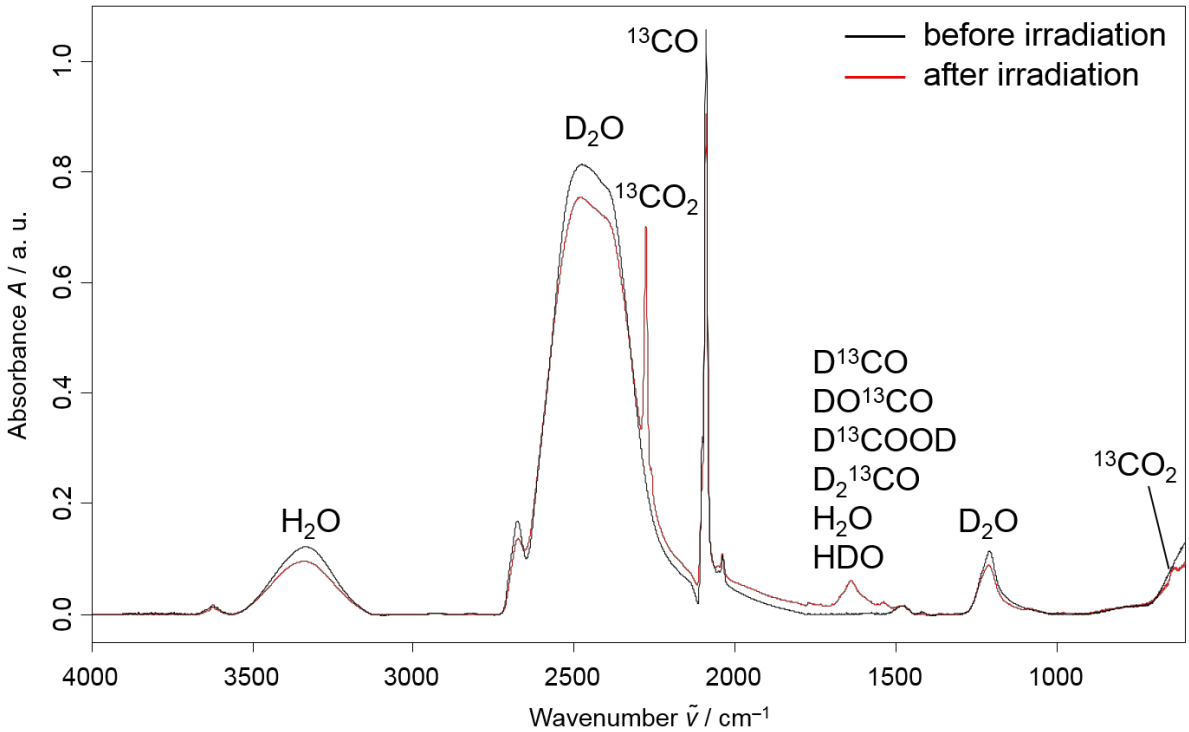

Figure S7: Recorded IR spectra of a deuterated water (D_2O) and ^{13}C-carbon monoxide (^{13}CO) ice before (black) and after (red) 2 h electron irradiation.

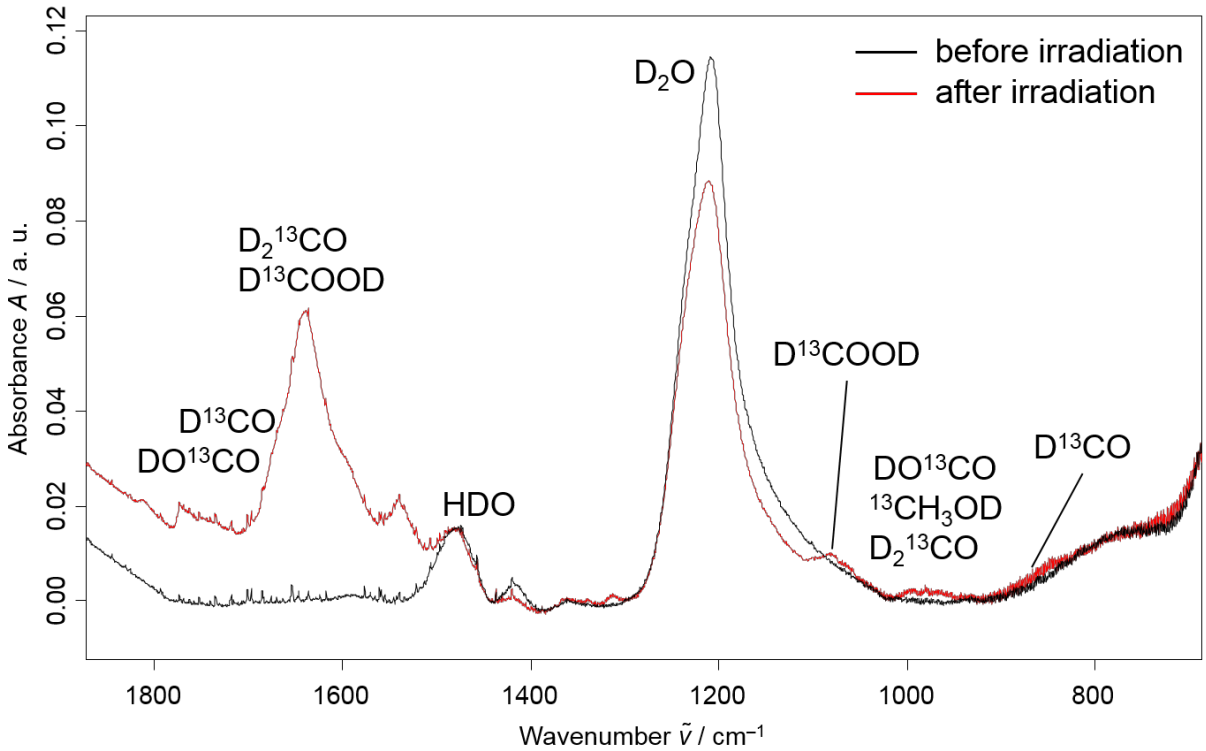

Figure S8: Recorded IR spectra of a deuterated water (D_2O) and ^{13}C-carbon monoxide (^{13}CO) ice before (black) and after (red) 2 h electron irradiation.

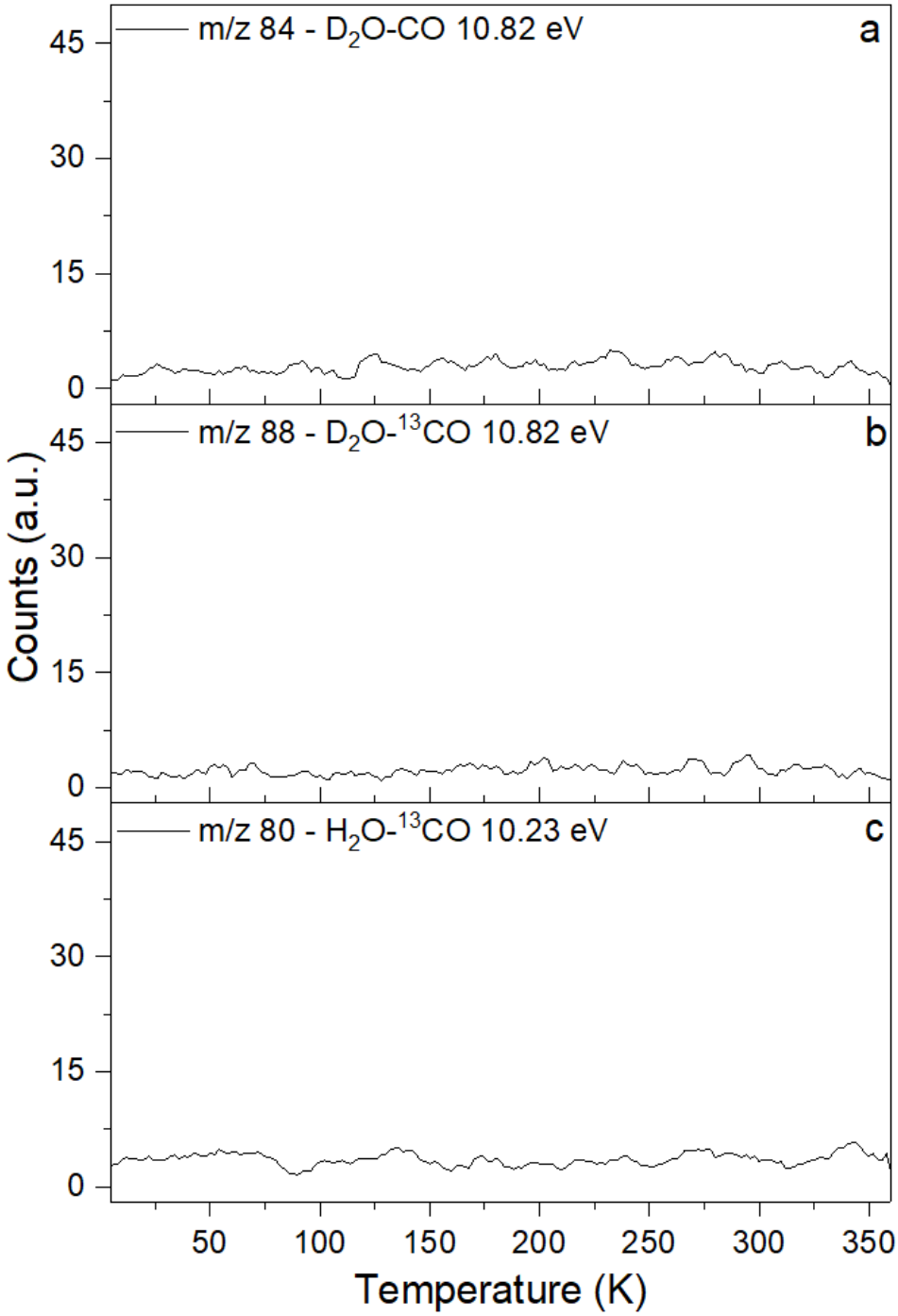

Figure S9: The absence of the signals from $C_4D_{10}O$ (a) and $^{13}C_4D_{10}O$ (b) isotopologues, as measured from the D_2O:CO and D_2O:^{13}CO experiments, respectively, reveals that $C_4H_{10}O$ isomers were not formed in the H_2O:CO experiments; (c) Absence of signal from *m/z* 80 collected at 10.23 eV in the H_2O:^{13}CO experiment reveals that $^{13}C_6H_2$, $^{13}CH_3O_4$, $^{13}C_2H_6O_3$, and/or O_5 were not detected in our study.

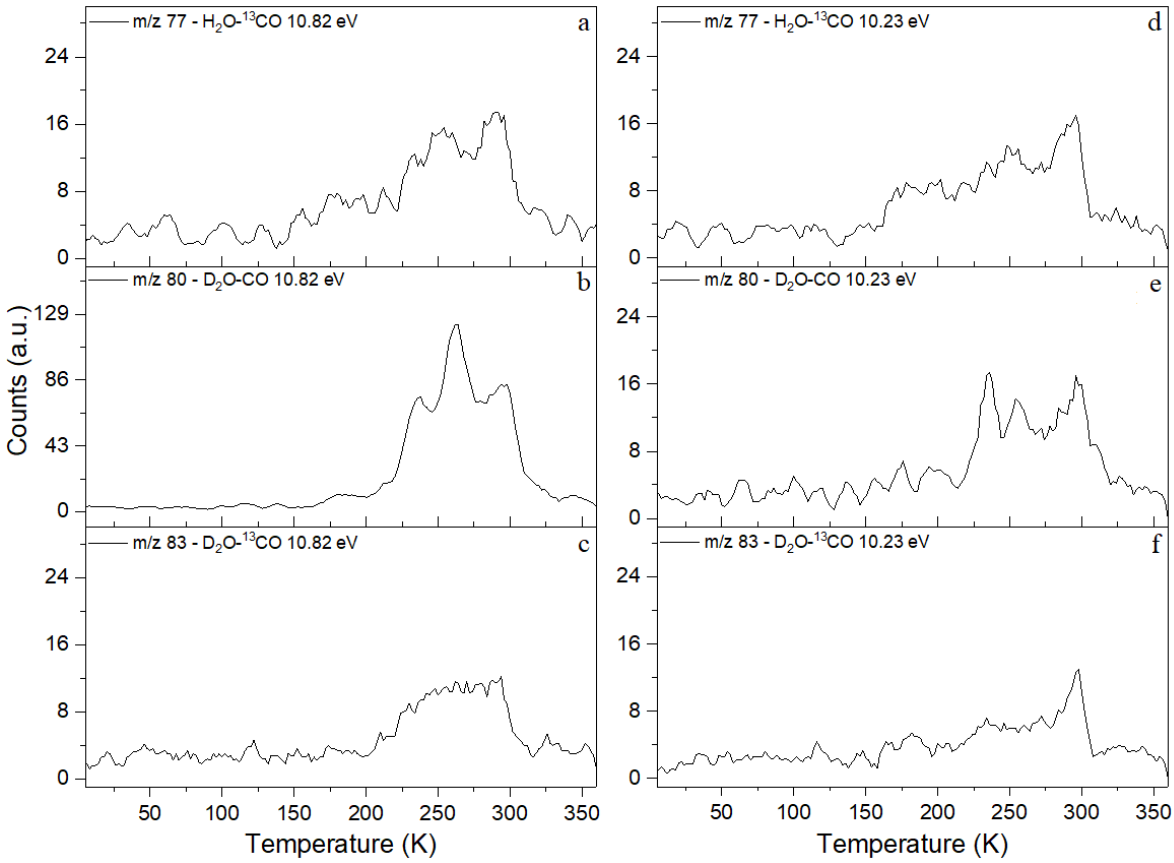

Figure S10: Potential signals from isotopologues of $C_3H_6O_2$ as measured in isotopically-labeled experiments at 10.82 eV (a, b, c) and at 10.23 eV (d, e, f).

Table S1: Identified IR signals and assignments of new products after irradiating a H_2O:CO ice.

$\tilde{\nu}_{exp.}$ / cm^{-1}	$\tilde{\nu}_{Lit.}$ / cm^{-1}	Assignment
~2345	2346[13]	ν_3 CO_2
~2327	2330[13]	ν_3 $OC^{18}O$
~2278	2281[13]	ν_3 $^{13}CO_2$
~1852	1853[14]	ν_3 HCO
~1839	1833[15]	ν_2 *trans*-HOCO
~1785	1797[15]	ν_2 *cis*-HOCO
~1718	1726[16]	ν_2 H_2CO
~1700	1767[17]	ν_3 HCOOH
~1499	1496[16]	ν_3 H_2CO
~1274	1273[13]	2 ν_2 CO_2
~1250	1245[16]	ν_5 H_2CO
~1224	1216[17]	ν_6 HCOOH
~1175	1171[16]	ν_6 H_2CO
~1095	1092[14]	ν_2 HCO
~1023	1031[14]	ν_8 CH_3OH
~661	660[13]	ν_2 CO_2

Table S2: Identified IR signals and assignments of new products after irradiating a D_2O:CO ice.

$\tilde{\nu}_{exp.}$ / cm^{-1}	$\tilde{\nu}_{Lit.}$ / cm^{-1}	Assignment
~2346	2346[13]	ν_3 CO_2
~2328	2330[13]	ν_3 $OC^{18}O$
~2280	2281[13]	ν_3 $^{13}CO_2$
~1789	1825[15]	ν_2 *trans*-DOCO
~1773	1798[15]	ν_2 *cis*-DOCO
~1735	1726[15]	ν_3 DCOOD
~1695	1695[15, 18]	ν_2 D_2CO
~1102	1103[18]	ν_3 D_2CO
~1072	1067[19]	ν_6 CD_3OD
~997	989[18]	ν_5 D_2CO
~852	853[15]	ν_2 DCO
~662	660[13]	ν_2 CO_2

Table S3: Identified IR signals and assignments of new products after irradiating a H_2O:^{13}CO ice.

$\tilde{\nu}_{exp.}$ / cm^{-1}	$\tilde{\nu}_{Lit.}$ / cm^{-1}	Assignment
~2346	2346[13]	ν_3 CO_2
~2280	2281[13]	ν_3 $^{13}CO_2$
~2328	2330[13]	ν_3 $OC^{18}O$
~1810	1821[18]	ν_3 $H^{13}CO$
~1800	1792[15]	ν_2 *trans*-$HO^{13}CO$
~1725	1756[15]	ν_2 *cis*-$HO^{13}CO$
~1693	1723[18]	ν_3 $H^{13}COOH$
~1660	1702[18]	ν_2 $H_2{}^{13}CO$
~1498	1505[18]	ν_3 $H_2{}^{13}CO$
~1204	1242[18]	ν_5 $H_2{}^{13}CO$
~1190	1170[18]	ν_6 $H_2{}^{13}CO$
~1095	1084[18]	ν_2 $H^{13}CO$
~1087	1091[18]	ν_6 $H^{13}COOH$
~1000	1010[20]	ν_8 $^{13}CH_3OH$
~638	639[21]	ν_2 $^{13}CO_2$

Table S4: Identified IR signals and assignments of new products after irradiating a D_2O:^{13}CO ice.

$\tilde{\nu}_{exp.}$ / cm^{-1}	$\tilde{\nu}_{Lit.}$ / cm^{-1}	$\Delta\tilde{\nu}_{exp.}$ / cm^{-1}	$\Delta\tilde{\nu}_{heor..}$ / cm^{-1}*	Assignment
~2280	2281[13]			ν_3 $^{13}CO_2$
~1770	-	69	51	ν_2 *trans*-$DO^{13}CO$
~1765	-	87	92	ν_3 $D^{13}CO$
~1640	-	60	74	ν_3 $D^{13}COOD$
~1640	-	78	79	ν_2 $D_2{}^{13}CO$
~1080	-	-	1162 (145)**	ν_6 $D^{13}COOD$
~1000	-	-	1094 (216)**	ν_3 *trans*-$DO^{13}CO$
~990	-	509	418	ν_3 $D_2{}^{13}CO$
~980	-	-	984 (39)**	ν_4 $^{13}CD_3OD$
~970	-	280	276	ν_5 $D_2{}^{13}CO$
~850	-	325	253	ν_2 $D^{13}CO$
~638	639[21]			ν_2 $^{13}CO_2$

* The theoretical harmonic isotope shifts were computed at B3LYP/cc-pVTZ level of theory.
** Absolute computed harmonic frequency (intensity in km mol^{-1}).

Table S5: Mass-shifts of the potential species detected at *m/z* = 74 in the water-carbon monoxide experiment upon isotopic substitution.

Formula	**Experiment**			
	H_2O:CO	**D_2O:CO**	**H_2O:^{13}CO**	**D_2O:^{13}CO**
$C_2H_2O_3$	74	76	76	78
$C_3H_6O_2$	74	80	77	83
$C_4H_{10}O$	74	84	78	88
C_6H_2	74	76	80	82

Column densities for CO and CO_2 were calculated according to one of our previous studies.[22]

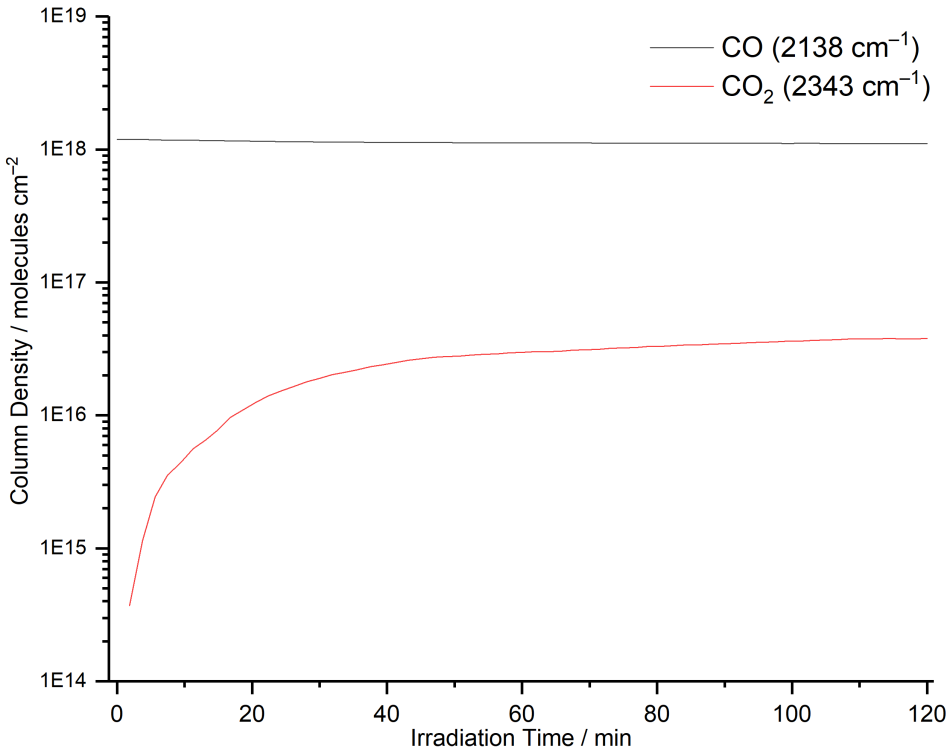

Figure S11: Change of the column density for CO and CO_2 over the irradiation time.

Table S6: Calculated column densities for CO and CO_2 before and after irradiation.

	IR-Peak / cm^{-1}	*A* / cm molecule^{-1}	*Area*$_{Int.}$ / cm^{-2}		*N* / molecules cm^{-2}	
			before irrad.	after irrad.	before irrad.	after irrad.
CO	2138	$1.12 \cdot 10^{-17}$[23]	16.32	15.25	$1.19 \cdot 10^{-18}$	$1.11 \cdot 10^{-18}$
CO_2	2343	$7.60 \cdot 10^{-17}$[23]	0.00	3.54	0	$3.79 \cdot 10^{-16}$

Based on these calculations the total CO conversion is 6.5%. Nearly every second CO molecule (48.9%) is transformed to CO_2.

Cartesian Coordinates for Selected Structures

MP2/cc-pVTZ optimized geometry (distances in Å), electronic energies (in hartree), zero-point vibrational energies (ZPVE), extrapolated CCSD(T)/CBS energies (in hartree) and adiabatic ionization energies (IE) at CCSD(T)/CBS//MP2/cc-pVTZ level of theory.

(*E,E*) glyoxylic acid (C_s)

C	–0.859006	–0.555222	0.000000
C	0.586807	–0.073210	0.000000
O	1.517032	–0.839497	0.000000
O	0.693086	1.258278	0.000000
H	–0.220165	1.597248	0.000000
O	–1.779488	0.237616	0.000000
H	–0.992400	–1.643363	0.000000

E[HF] = –301.5964898
E[MP2] = –302.6028233
E[CCSD(T)/cc-pVDZ] = –302.3521374
E[CCSD(T)/cc-pVTZ] = –302.6511254
E[CCSD(T)/cc-pVQZ] = –302.7444269
E[CCSD(T)/CBS] = –302.7867494
ZPVE = 27.4547 kcal mol^{-1}

(*E,E*) glyoxylic acid cation (C_s)

C	–1.044516	–0.627091	0.000000
C	0.746497	0.022319	0.000000
O	1.471952	–0.881670	0.000000
O	0.750281	1.302387	0.000000
H	–0.132607	1.716836	0.000000
O	–1.879603	0.174832	0.000000
H	–0.966137	–1.725761	0.000000

E[HF] = –301.2312687
E[MP2] = –302.2173965
E[CCSD(T)/cc-pVDZ] = –301.9799916
E[CCSD(T)/cc-pVTZ] = –302.2661924
E[CCSD(T)/cc-pVQZ] = –302.3552142
E[CCSD(T)/CBS] = –302.3954055
ZPVE = 27.1143 kcal mol^{-1}

Adiabatic IE: 10.63 eV

(*E,Z*) glyoxylic acid (C_s)

C	–0.728148	–0.756602	0.000000
C	0.003256	0.578617	0.000000
O	–0.598519	1.628358	0.000000
O	1.333938	0.442732	0.000000
H	1.694167	1.342655	0.000000
O	–0.173304	–1.829603	0.000000
H	–1.820701	–0.632588	0.000000

E[HF] = –301.5961413
E[MP2] = –302.6005130
E[CCSD(T)/cc-pVDZ] = –302.3506021
E[CCSD(T)/cc-pVTZ] = –302.6488887
E[CCSD(T)/cc-pVQZ] = –302.7420272
E[CCSD(T)/CBS] = –302.7843127
ZPVE = 27.1818 kcal mol^{-1}

(*E,Z*) glyoxylic acid cation (C_s)

C	–0.656096	–1.042367	0.000000
C	–0.027365	0.776692	0.000000
O	–0.916818	1.550392	0.000000
O	1.245634	0.670545	0.000000
H	1.687229	1.547160	0.000000
O	0.192383	–1.801416	0.000000
H	–1.748664	–0.957845	0.000000

E[HF] = –301.2348124
E[MP2] = –302.2178562
E[CCSD(T)/cc-pVDZ] = –301.9819678
E[CCSD(T)/cc-pVTZ] = –302.2674128
E[CCSD(T)/cc-pVQZ] = –302.3562207
E[CCSD(T)/CBS] = –302.3963293
ZPVE = 26.5854 kcal mol^{-1}

Adiabatic IE: 10.53 eV

(*Z,Z*) glyoxylic acid (C_s)

C	–0.742664	–0.790187	0.000000
C	0.036221	0.525191	0.000000
O	1.235373	0.620192	0.000000
O	–0.831474	1.559258	0.000000
H	–0.295588	2.366836	0.000000
O	–0.175113	–1.856142	0.000000
H	–1.837368	–0.690013	0.000000

E[HF] = –301.5933634
E[MP2] = –302.5987173
E[CCSD(T)/cc-pVDZ] = –302.3487107
E[CCSD(T)/cc-pVTZ] = –302.6469385
E[CCSD(T)/cc-pVQZ] = –302.7400880
E[CCSD(T)/CBS] = –302.7823978
ZPVE = 27.0773 kcal mol^{-1}

(*Z,Z*) glyoxylic acid cation (C_s)

C	–0.718530	–1.037433	0.000000
C	–0.009850	0.697710	0.000000
O	–0.843972	1.531869	0.000000
O	1.264706	0.534145	0.000000
H	1.750044	1.386643	0.000000
O	–1.849974	–1.176996	0.000000
H	0.213911	–1.625006	0.000000

E[HF] = –301.2296387
E[MP2] = –302.2175597
E[CCSD(T)/cc-pVDZ] = –301.9804133
E[CCSD(T)/cc-pVTZ] = –302.2655284
E[CCSD(T)/cc-pVQZ] = –302.3542000
E[CCSD(T)/CBS] = –302.3942250
ZPVE = 30.8872 kcal mol^{-1}

Adiabatic IE: 10.73 eV

formic anhydride **11** (C_s)

C	0.081641	2.332282	0.000000
O	0.028409	0.960617	0.000000
O	–0.855299	3.079812	0.000000
H	1.132286	2.629039	0.000000
C	–1.231023	0.371276	0.000000
O	–1.338102	–0.816632	0.000000
H	–2.038627	1.102854	0.000000

E[HF] = –301.6030359
E[MP2] = –302.6049819
E[CCSD(T)/cc-pVDZ] = –302.3544709
E[CCSD(T)/cc-pVTZ] = –302.6533150
E[CCSD(T)/cc-pVQZ] = –302.7458979
E[CCSD(T)/CBS] = –302.7874549
ZPVE = 27.0089 kcal mol^{-1}

formic anhydride cation (C_s)

C	–1.450264	0.295482	0.000000
O	0.106762	0.749381	0.000000
O	–1.711343	–0.831246	0.000000
H	–1.958362	1.255017	0.000000
C	0.921358	–0.208802	0.000000
O	2.170523	–0.018932	0.000000
H	0.623309	–1.266946	0.000000

E[HF] = –301.2515921
E[MP2] = –302.1906032
E[CCSD(T)/cc-pVDZ] = –301.9674119
E[CCSD(T)/cc-pVTZ] = –302.2506445
E[CCSD(T)/cc-pVQZ] = –302.3377107
E[CCSD(T)/CBS] = –302.3763540
ZPVE = 25.6503 kcal mol^{-1}

Adiabatic IE: 11.43 eV

formic anhydride **11'** (C_1)

C	1.199963	0.317967	0.066444
O	0.000000	1.006817	0.000000
O	1.385720	–0.814291	–0.258139
H	1.956984	1.018709	0.426596
C	–1.199963	0.317966	–0.066444
O	–1.385719	–0.814292	0.258139
H	–1.956985	1.018708	–0.426596

HF = –301.5972704
MP2 = –302.6007522
E[CCSD(T)/cc-pVDZ] = –302.3505691
E[CCSD(T)/cc-pVTZ] = –302.6486706
E[CCSD(T)/cc-pVQZ] = –302.7412534
E[CCSD(T)/CBS] = –302.7829604
ZPVE = 26.8608 kcal mol^{-1}

formic anhydride cation 1 (C_{2v})

C	–1.111945	0.000000	0.339411
O	0.000000	0.000000	1.113650
O	–1.042052	0.000000	–0.868438
H	–2.045651	0.000000	0.904216
C	1.111944	0.000000	0.339411
O	1.042052	0.000000	–0.868438
H	2.045651	0.000000	0.904216

HF = –301.2325749
MP2 = –302.2057720
E[CCSD(T)/cc-pVDZ] = –301.9793279
E[CCSD(T)/cc-pVTZ] = –302.2648551
E[CCSD(T)/cc-pVQZ] = –302.3529757
E[CCSD(T)/CBS] = –302.3923120
ZPVE = 32.5685 kcal mol^{-1}

Adiabatic IE: 10.88 eV

formic anhydride **11''** (C_{2v})

C	0.033157	2.346639	0.000000
O	0.026148	0.970361	0.000000
O	1.050201	2.969061	0.000000
H	–0.973011	2.782164	0.000000
C	–1.206858	0.358897	0.000000
O	–1.318671	–0.828236	0.000000
H	–2.040445	1.071069	0.000000

E[HF] = –301.5961684
E[MP2] = –302.6004857
E[CCSD(T)/cc-pVDZ] = –302.3487333
E[CCSD(T)/cc-pVTZ] = –302.6483839
E[CCSD(T)/cc-pVQZ] = –302.7409569
E[CCSD(T)/CBS] = –302.7823412
ZPVE = 26.9175 kcal mol^{-1}

formic anhydride cation 3 (C_{2v})

C	0.000000	–1.155376	–0.337306
O	0.000000	0.000000	0.392471
O	0.000000	–2.179915	0.267949
H	0.000000	–1.067891	–1.435164
C	0.000000	1.155376	–0.337306
O	0.000000	2.179915	0.267949
H	0.000000	1.067891	–1.435164

E[HF] = –301.1783402
E[MP2] = –302.1758232
E[CCSD(T)/cc-pVDZ] = –301.9446795
E[CCSD(T)/cc-pVTZ] = –302.2298821
E[CCSD(T)/cc-pVQZ] = –302.3172733
E[CCSD(T)/CBS] = –302.3558819
ZPVE = 27.2307 kcal mol^{-1}

Adiabatic IE: 11.62 eV

References and Full Gaussian 16 Citation

Gaussian 16:

Gaussian 16, Revision A.03; Frisch, M. J.; Trucks, G. W.; Schlegel, H. B.; Scuseria, G. E.; Robb, M. A.; Cheeseman, J. R.; Scalmani, G.; Barone, V.; Petersson, G. A.; Nakatsuji, H.; Li, X.; Caricato, M.; Marenich, A. V.; Bloino, J.; Janesko, B. G.; Gomperts, R.; Mennucci, B.; Hratchian, H. P.; Ortiz, J. V.; Izmaylov, A. F.; Sonnenberg, J. L.; Williams-Young, D.; Ding, F.; Lipparini, F.; Egidi, F.; Goings, J.; Peng, B.; Petrone, A.; Henderson, T.; Ranasinghe, D.; Zakrzewski, V. G.; Gao, J.; Rega, N.; Zheng, G.; Liang, W.; Hada, M.; Ehara, M.; Toyota, K.; Fukuda, R.; Hasegawa, J.; Ishida, M.; Nakajima, T.; Honda, Y.; Kitao, O.; Nakai, H.; Vreven, T.; Throssell, K.; Montgomery, J. A., Jr.; Peralta, J. E.; Ogliaro, F.; Bearpark, M. J.; Heyd, J. J.; Brothers, E. N.; Kudin, K. N.; Staroverov, V. N.; Keith, T. A.; Kobayashi, R.; Normand, J.; Raghavachari, K.; Rendell, A. P.; Burant, J. C.; Iyengar, S. S.; Tomasi, J.; Cossi, M.; Millam, J. M.; Klene, M.; Adamo, C.; Cammi, R.; Ochterski, J. W.; Martin, R. L.; Morokuma, K.; Farkas, O.; Foresman, J. B.; Fox, D. J., Gaussian Inc., Wallingford CT **2016**.

[1] a) A. Bergantini, S. Góbi, M. J. Abplanalp, R. I. Kaiser, *Astrophys. J.* **2018**, *852*, 70; b) S. Góbi, A. Bergantini, A. M. Turner, R. I. Kaiser, *J. Phys. Chem. A* **2017**, *121*, 3879-3890.
[2] R. I. Kaiser, S. Maity, B. M. Jones, *Phys. Chem. Chem. Phys.* **2014**, *16*, 3399-3424.
[3] A. Bergantini, B. G. Nair, N. J. Mason, H. J. Fraser, *A&A* **2014**, *570*, A120.
[4] R. I. Kaiser, S. Maity, B. M. Jones, *PCCP* **2014**, *16*, 3399-3424.
[5] D. Drouin, A. R. Couture, D. Joly, X. Tastet, V. Aimez, R. Gauvin, *Scanning* **2007**, *29*, 92-101.
[6] A. Yeghikyan, *Ap* **2011**, *54*, 87-99.
[7] B. M. Jones, R. I. Kaiser, *J. Phys. Chem. Lett.* **2013**, *4*, 1965-1971.
[8] a) R. I. Kaiser, G. Eich, A. Gabrysch, K. Roessler, *Astrophys. J.* **1997**, *484*, 487-498; b) R. I. Kaiser, A. Gabrysch, K. Roessler, *Rev. Sci. Instrum.* **1995**, *66*, 3058-3066.
[9] C. Møller, M. S. Plesset, *Phys. Rev.* **1934**, *46*, 618-622.
[10] J. Dunning, Thom H., *J. Chem. Phys.* **1989**, *90*, 1007-1023.
[11] a) J. Čížek, *J. Chem. Phys.* **1966**, *45*, 4256-4266; b) R. J. Bartlett, J. D. Watts, S. A. Kucharski, J. Noga, *Chem. Phys. Lett.* **1990**, *165*, 513-522; c) K. Raghavachari, *Annu. Rev. Phys. Chem.* **1991**, *42*, 615-642; d) J. F. Stanton, *Chem. Phys. Lett.* **1997**, *281*, 130-134.
[12] K. A. Peterson, D. E. Woon, T. H. Dunning, *J. Chem. Phys.* **1994**, *100*, 7410-7415.
[13] C. S. Jamieson, A. M. Mebel, R. I. Kaiser, *Astrophys. J. S.* **2006**, *163*, 184-206.
[14] C. J. Bennett, R. I. Kaiser, *Astrophys. J.* **2007**, *660*, 1289-1295.
[15] D. E. Milligan, M. E. Jacox, *J. Chem. Phys.* **1971**, *54*, 927-942.
[16] C. J. Bennett, S.-H. Chen, B.-J. Sun, A. H. H. Chang, R. I. Kaiser, *Astrophys. J.* **2007**, *660*, 1588-1608.
[17] M. Pettersson, J. Lundell, L. Khriachtchev, M. Räsänen, *J. Am. Chem. Soc.* **1997**, *119*, 11715-11716.
[18] T. L. Tso, E. K. C. Lee, *J. Phys. Chem.* **1984**, *88*, 5475-5482.
[19] H. Hidaka, A. Kouchi, N. Watanabe, *J. Chem. Phys.* **2007**, *126*, 204707.
[20] S. Maity, R. I. Kaiser, B. M. Jones, *Faraday Discuss.* **2014**, *168*, 485-516.
[21] C. J. Bennett, C. S. Jamieson, R. I. Kaiser, *Phys. Chem. Chem. Phys.* **2010**, *12*, 4032-4050.
[22] A. M. Turner, M. J. Abplanalp, S. Y. Chen, Y. T. Chen, A. H. H. Chang, R. I. Kaiser, *Phys. Chem. Chem. Phys.* **2015**, *17*, 27281-27291.
[23] A. Jolly, H. Cottin, M. Bouilloud, M.-C. Gazeau, N. Fray, Y. Bénilan, *Mon. Not. R. Astron. Soc.* **2015**, *451*, 2145-2160.